International Journal of Mechanical Sciences 274 (2024) 109235

Contents lists available at ScienceDirect

International Journal of Mechanical Sciences

journal homepage: www.elsevier.com/locate/ijmecsci

Stiffness and pre-stretching estimation from indentation test of hyperelastic membrane

T. Fąs, K. Kazimierska-Drobny, M. Kaczmarek *

Kazimierz Wielki University, Kopernika 1, Bydgoszcz 85-074, Poland

ARTICLE INFO

Keywords:
Membrane
Indentation
Parameter identification
Stiffness
Pre-stretching
Elastomers

ABSTRACT

Obtaining precise data on the mechanical properties of soft materials, often in the form of thin, pre-tensioned membranes, is crucial, especially when conventional testing methods have limited applicability. The article focuses on an innovative method for estimating the Young's modulus and pre-stretching the membranes using the indentation method, assuming an isotropic, incompressible hyperelastic material. The parameters were estimated for two models of indenter-membrane contact: with perfect slip and without slip. Experimental tests were performed for pre-stretched latex membranes glued to a stiffer ring to minimize the effect of attachment on membrane deformation. In order to validate the estimation method, the predictions of the model with the determined mechanical parameters were compared with the results of indentation tests with a liquid layer under the membrane. The discussion shows the consistency of the estimation results with the literature results for small latex deformations, and indicates the advantages and numerous limitations of the approach, especially related to the choice of the material model.

1. Introduction

Indentation tests are a frequently used alternative to testing the mechanical properties of materials which, for various reasons, such as the availability or application in the form of thin films or the need for *in vivo* testing, are difficult to test in the form of classic samples used in the case of construction materials. This applies in particular to soft biological materials, such as skin, cell walls as well as thin layers of technical materials, such as elastomers [1–10]. Attention in this work is focused on elastomers, which are materials with a complex structure and non-standard mechanical properties. The constantly expanding range of elastomers available on the market means that new methods for their testing are needed in order to control quality, assess the properties of the newly created products and explain the causes of possible defects [11–18]. While performing indentation experiments is not difficult, the interpretation of the results of such tests, including the conversion of experimental data into mechanical parameters, requires the use of an appropriate and often complex model [8,19–22]. A model that can be used for thin layers of materials is the membrane model.

The theoretical analysis of the problem of a membrane subject to significant deformations was initiated in the 1940s by Rivlin and co-authors [23]. Works from that time have been collected and published [24]. The authors of this paper refer to the model formulated by Long et al. [25,26], which takes into account the presence of pre-stretch in the membrane. The proposed method is based on the assumption that biaxial elastomer stretching can provide more reliable data than the standard uniaxial tensile test, [7,27–29]. While uniaxial stretching has been standardized [30], biaxial methods are still not standardized and further improvement is recommended [27].

In the literature, we can find many publications devoted to advanced methods of membrane testing. For example, in [31] a two-axis tensioning device for study sheets of polymers with anisotropic properties was proposed. The work [25] presents the validation of the method of testing a round membrane under the pressure of the injected gas (bubble-inflation-technique). In [26], during a similar test, the fatigue load and the recording of the test by the vision system were taken into account. In [32], an analysis of the method based on biaxial stretching of cruciform specimens samples was carried out. In [13,33], the influence of changes in the geometry of the sample on the test results was checked. In [7,34], uniaxial and biaxial tensile tests were compared on the same sample.

This article develops an indentation method in an attempt to identify the Young's modulus and pre-stretch of the membrane, assuming that the membrane material has the properties of an incompressible,

* Corresponding author.
E-mail address: mkk@ukw.edu.pl (M. Kaczmarek).

https://doi.org/10.1016/j.ijmecsci.2024.109235
Received 10 January 2024; Received in revised form 25 March 2024; Accepted 26 March 2024
Available online 31 March 2024

isotropic neoHookean material. The source of the data for identification were tests on a circular, initially flat membrane using a cylindrical flat-ended indenter. It was assumed that the diameter of the membrane would be much larger than the diameter of the indenter and the indentation depth would not exceed the diameter of the indenter. Such assumptions ensure that the contact of the membrane with the indenter occurs only on its face. It is assumed that there are no wrinkles on the membrane and that it is impermeable to liquids.

Due to the friction between the indenter and the membrane, the deformation distribution of the membrane under the indenter cannot be clearly predicted. For this reason, it was decided to estimate the parameters using two extreme model assumptions for the membrane-indenter contact: one with perfect slip of the membrane on the indenter (slip contact) and one that excludes slipping over the entire surface contact (stick contact). All other scenarios where slippage occurs in part of the contact surface, assuming axial deformation symmetry, will be within the limits of the predictions for the considered extreme cases.

In order to validate the method, the results of tests with a layer of water under the membrane were used, assuming that the volume of the liquid does not change. The quantities that were measured and used for validation were the force acting on the indenter and the liquid pressure. In the discussion, the obtained identification results were compared with the results available from the literature, and the possibilities of developing the method were indicated.

2. Materials and test method

Latex membranes with various initial stretches (pre-stretches) were used for the tests. The membranes were obtained by cutting circular samples from one of the available rehabilitation bands (Qmed, MDH Sp. z o.o., Poland). The average thickness of the tested band before deformation was determined on the basis of measurements with a micrometer screw and was equal to 0.285 mm. The method of preparing the pre-stretched membranes is schematically shown in Fig. 1 and the station used for stretching the membranes is shown in Fig. 3a. First, the free band was attached to the stand by the clamping of an aluminum rings with an internal diameter of 130 mm. The membrane was tensioned by pressing the conical plastic piston to a controlled depth (h), measured with a caliper integrated with the stand. The force exerted by the piston on membrane F_p, referred to here as the pre-stretching force, was measured with a dynamometer (Sauter FL). The pre-stretched membrane was then bonded on with quick-drying epoxy glue to a plastic ring made with a 3D printing technique. The ring, with an inner diameter of 100 mm and an outer diameter of 120 mm, was pressed against the membrane by force *Fc* (weight approx. 2 kg). When the adhesive bonds the stretched membrane to the ring, the rest of the band was cut off at the outer circumference of the ring. Membranes with various initial stretches were prepared for the tests with a pre-stretching force of up to 30 N.

The bonding of the stretched membrane to the ring prevented the membrane from slipping out of the mounting bracket without applying significant compressive force. The use of lower compressive forces, in turn, reduced the occurrence of undesirable deformations of the membrane not resulting from the pressure of the indenter. In the preliminary tests, when samples without ring bonding were mounted directly in the holder, such deformations and characteristic wrinkles were observed around the inner edge of the mounting holder. The solution of bonding the membrane to the ring using glue was an alternative to the method of making membranes together with a ring of much greater thickness than the membrane by casting such a sample in a suitable mold, see [35].

The measuring system for quasi-static indentation tests of membranes is shown schematically in Fig. 2 and the appearance of its main components is shown in Fig. 3b. The stand consisted of a universal screw mechanism, an integrated caliper, a dynamometer (Sauter FL) equipped with a cylindrical steel indenter with a diameter of 10 mm, a liquid pressure sensor (DO-10P, Wika) under the membrane, a membrane mounting system from the water chamber and a computer not shown in Fig. 2.

The penetration of the indenter was carried out in 10 steps every 1 mm with a time of about 1 s per step and with intervals between steps of about 10 s. For each case, the tests were performed 2 or 3 times, first increasing the penetration and then withdrawing the indenter with the same indentation step. The indentation tests were carried out in two configurations: on membranes stretched in the air and on membranes under which there was water in a sealed chamber. In both cases, the quantity manipulated and measured with a caliper was the penetration of the indenter into the membrane, with the force response to the indenter being measured using a dynamometer. In tests with water under the membrane, the pressure of the liquid was additionally measured.

Taking into account the geometrical parameters of the tests (membrane diameter 100 mm, indenter diameter 10 mm and maximum

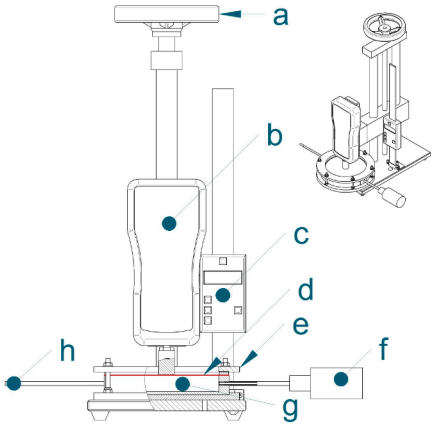

Fig. 2. Scheme of the measuring device: a - universal screw mechanism, b - dynamometer, c - caliper, d - membrane, e - membrane fastening system, f - pressure sensor, g - place for the liquid, h - liquid delivery channel.

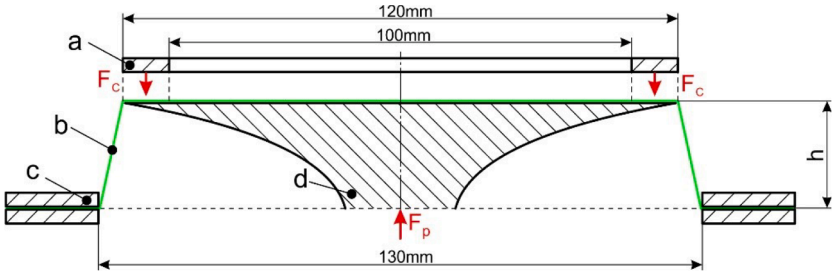

Fig. 1. Diagram showing the tensioning and fixing of the membrane to the ring: a – ring (bonded to the membrane); b - membrane; c – aluminum rings; d – piston; F_p – pre-stretching force, F_c – clamping force on the ring.

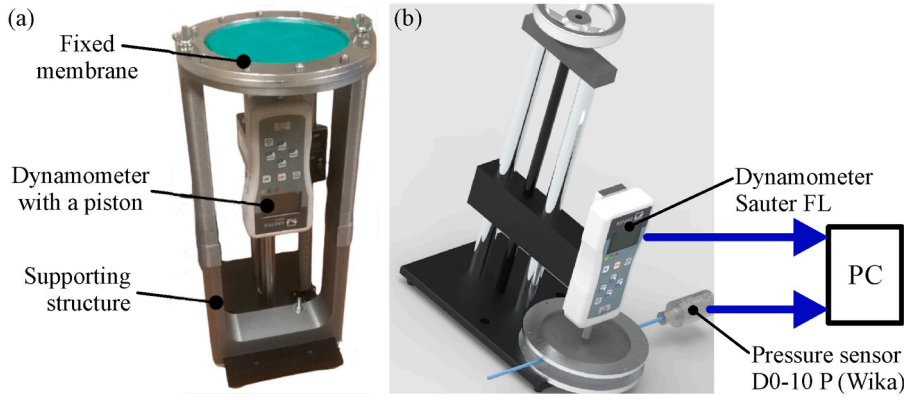

Fig. 3. Equipment for tensioning the membranes (a) and testing the membrane with the indentation method (b).

penetration depth 10 mm), the model considerations could be limited to a situation where the contact of the membrane with the indenter occurred only on its front surface. Research in this range of penetration greatly simplifies the modeling of membrane deformation.

3. Solution methods

The membrane model corresponding to the experimental tests performed is presented in Appendix A. Determination of Young's modulus E and pre-stretching λ_p is carried out on the basis of quasi-static indentation test data for the case where there is no liquid under the membrane. In paper [36] it was shown that the solution of Eq. (A1) with boundary conditions (A4)–(A8) for the case of a membrane with a liquid is effectively obtained using the Runge-Kutta method based on Lobatto quadrature formula. This method is used here to solve the problem both for the membrane without liquid and with liquid under the membrane.

The least squares method is used to identify the parameters E and λ_p. These parameters can be found by minimizing the following objective function:

$$\chi^2(E,\lambda_p) = \sum_{i=ni}^{n} \left[\frac{F_i - \underline{F}_i(E,\lambda_p)}{\sigma_{Fi}} \right]^2 \tag{1}$$

where F_i are the values of the measured forces in the experiment and $\underline{F}_i$ are the forces determined from the model for indentation depth z_{0i}, while σ_{Fi} denotes the standard uncertainty of the measurement of forces F_i. The local minimization technique, known as the trust region dogleg method, is used here, and requires defining constraints. The lower and upper bounds of the Young's modulus were defined based on the available data for latex. The upper limit of the pre-stretch value was set by taking an appropriate margin in relation to the stretch implemented during the preparation of the membranes.

The summation of the squared residuals in Eq. (1) is from ni to n. The upper index n is the number of measurements (registered forces) in a single test, and the lower index ni indicates the smallest force taken for analysis. In all calculations, ni=4 was assumed, which means that data with a depth of 4 to 10 mm were taken into account. The omission of smaller force values in the objective function results from the observed instability of the numerical procedure integrating the membrane model for small penetration depths. In order to determine the forces from the model in a single iteration of optimization calculations, it was assumed that the pressure in the liquid present in the system of Eq. (A1) was equal to zero and the contact conditions between the membrane and the indenter were of the slip or stick type, resulting in the appropriate boundary conditions (see Appendix A). The coefficient of determination R^2 was used to assess the quality of the fit of the experimental results by the model predictions. All codes (finding identified parameters and integrating models) were written in the Matlab environment (version R2009b).

4. Results and discussion

The section presents sample results of an indentation test of latex membranes with different pre-stretching tested without water and with water under the membrane. These results were used as data for estimation of Young's modulus and membrane pre-stretch and method validation, respectively. The section also includes an analysis of the uncertainty of parameter identification and a discussion of the results indicating the advantages and limitations of the proposed method in the context of other works.

4.1. Sample results of indentation tests

The tests were carried out using latex membranes with various degrees of initial stretching caused by the force, the maximum value of which was 30 N. In all cases, the membrane deformations were carried out repeatedly in the range of relatively small deformations, which minimizes the occurrence of the Mullins effect [37,38].

Fig. 4 shows the results in the form of force dependence as a function of penetration of the indenter into the membrane in the process of insertion and retraction of the indenter for 3 membranes with pre-stretching caused by pre-stretching forces of 0, 18 and 28 N and without water under the membrane.

Fig. 5 shows the results showing the force and water pressure depending on the depth of the indenter for the same membranes when the space under the membrane is filled with water of constant volume.

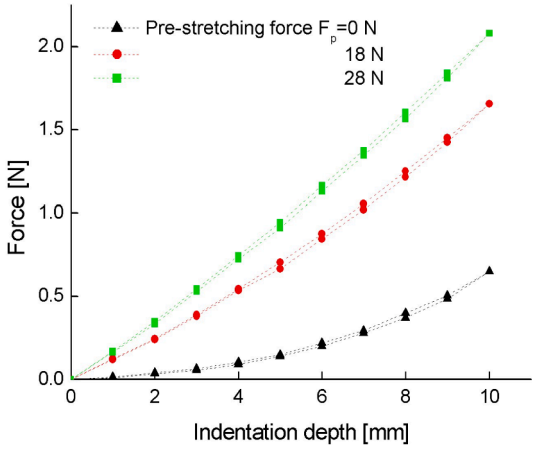

Fig. 4. Force dependence on indenter depth for membrane pre-stretching force F_p=0, 18 and 28 N without water under the membrane.

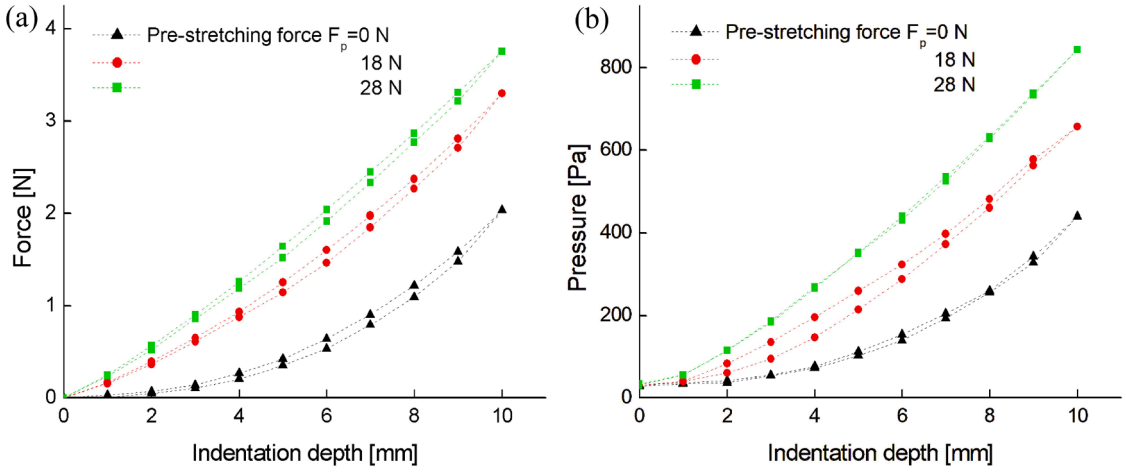

Fig. 5. Dependence of the force (a) and pressure (b) of the liquid on the depth of the indenter for a membrane with a liquid for membranes with pre-stretching force $F_p = 0$, 18, 28 N.

In both tests (with and without water under the membrane) a slight hysteresis is observed in the force versus penetration depth plot, despite the slow loading and unloading of the membrane. The pressure in the water takes a similar course.

4.2. Identification results

In accordance with the procedure described in paragraph 3, the identification of Young's modulus E and pre-stretch λ_p was carried out. As the input data, the vector of forces for a set of indentation depths z_{0i}were used. The values of uncertainty of measurement of the force u_{Fi} are assumed to be independent of the indentation depth, allowing its presence to be neglected in Formula (1). The results of the estimation together with the values of the coefficient of determination R^2 for different values of the pre-stretching force and both considered contact conditions of the membrane and the indenter (slip, stick) are included in Table 1 and illustrated in Figs. 6 and 7.

The results of estimation of Young's modulus for the membranes with different pre-stretching forces show noticeable differences in the values obtained when using the stick or slip contact model. In general, however, greater discrepancies are seen between the results obtained on the basis of tests using membranes with different pre-stretches. The average Young's modulus values were 2.22 MPa for stick contact and 2.36 MPa for slip contact.

The results of the estimation of the pre-stretching λ_p of the membrane show an approximately linear relationship with the pre-stretching force, see Fig. 7. At the same time, there is a slight difference in the results obtained for slip and stick contact. The graph shown in Fig. 7 additionally shows two results measured directly from the membrane using a measuring tape with a millimeter scale. The diameters of the circles drawn on the membrane, marked with a permanent marker before stretching and after stretching, and bonding the membrane to the ring. The pre-stretching values determined are 1.066 and 1.116, respectively, for the pre-stretching force of 18 and 28 N, and these values are comparable to the stretches determined indirectly in the optimization process.

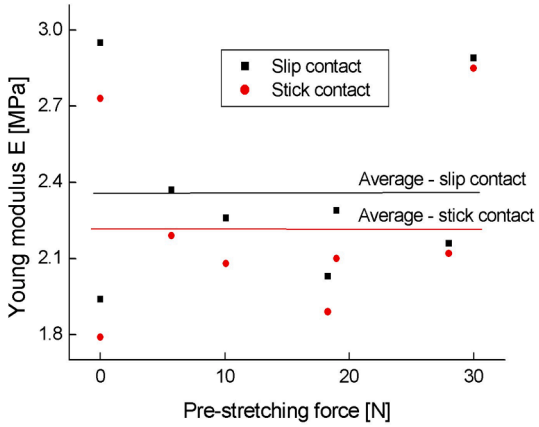

Fig. 6. Young's modulus values of the membrane material for various pre-stretching forces and contact conditions.

The values of the coefficient of determination R^2 presented in Table 1 indicate a good agreement of the predictions of the model containing the determined values of modulus E and pre-stretch λ_p for both the slip and

Table 1
Results of identification of Young's modulus E and pre-stretching $\lambda_p$together with the values of the coefficient of determination R^2 for different values of pre-stretching force and contact conditions of the membrane and the indenter (slip, stick).

Pre-stretching force F_p[N]	Membrane thickness [mm]	Results for slip contact			Results for stick contact		
		Young's moduli E [MPa]	Pre-stretch λ_p [-]	R^2	Young's moduli E [MPa]	Pre-stretch λ_p [-]	R^2
0	0.285	1.94	1.0057	0.996	1.79	1.006	0.996
0	0.285	2.95	1.005	0.998	2.73	1.005	0.998
5.7	0.27	2.37	1.014	0.99	2.19	1.016	0.99
10.1	0.26	2.26	1.026	0.98	2.08	1.029	0.982
18.3	0.235	2.03	1.061	0.975	1.86	1.068	0.975
19	0.22	2.29	1.068	0.97	2.1	1.076	0.97
28	0.21	2.16	1.099	0.97	2.12	1.099	0.97
30	0.2	2.89	1.099	0.97	2.85	1.099	0.97

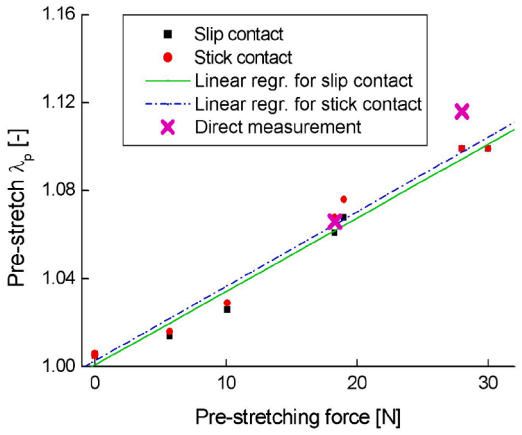

Fig. 7. Membrane pre-stretch values λ_p [-] for different pre-stretching force and contact conditions and corresponding regression lines.

stick contact conditions with the experimental results. This is confirmed by the graph in Fig. 8a, which presents example results of the experiments and modeling for membranes with pre-stretching forces of 10 and 19 N. The fit quality turns out to be independent of the indenter-membrane contact condition.

In order to assess the uniqueness of the results of the optimization procedure, repeated identification attempts were made with different starting points for E and λ_p. An example showing the results of such tests for a membrane with a pre-stretching force 19 N is shown in Fig. 8b.

Lines connect the starting points (starting values of Young's modulus and initial stretch) and the result values obtained from the identification procedure. It can be seen that for the considered range of starting parameter values, the identification result is unambiguous, which indicates the existence of one minimum of the objective function.

4.3. Uncertainty analysis

The evaluation of standard uncertainties of directly measured quantities x_i, i.e. displacement z_0, force F, membrane thickness h_0 and liquid pressure p was made on the basis of procedure type B [39] according to the formula $u_{xi} = \sqrt{\frac{a^2}{3}}$ where $2a$ is the difference between the bounds of x_i. In the case of measuring the indentation depth with a caliper, the reaction force of the membrane with a dynamometer and the thickness of the membrane with a micrometer, the resolution of the measuring apparatus was adopted as the value $2a$, while for the measurement of pressure the limit uncertainty was assumed, determined on the basis of the product of class of the apparatus and the measuring range, divided by 100.

The resolutions of the caliper, dynamometer and micrometer are respectively: 0.1 mm and 0.02 N and 0.01 mm. The class and range of the pressure gauge are 0.1 % and 25 kPa respectively. Finally, the uncertainties of the measurement of displacement z_0, force F, membrane thickness h_0 and liquid pressure p are 0.029 mm, 0.0058 N, 0.0029 mm and 14.4 Pa, respectively.

Uncertainty of the identified parameters: Young's modulus and pre-stretch are estimated on the basis of the calculation procedure adopted for non-linear problems solved by the least squares method [40]. According to this procedure, first a curvature matrix is determined, and the components of which are calculated according to the formula:

$$\alpha_{kl} = \sum_{i=ni}^{n} u_{Fi}^{\frac{1}{2}} \left[\frac{\partial F_i}{\partial a_k} \frac{\partial F_i}{\partial a_l} \right] \tag{2}$$

where a_k and a_l denote the identified parameters E (if k or $l = 1$) and λ_p (if k or $l = 2$), and the standard uncertainty of force measurement u_{Fi}, according to the previously adopted assumption, is a constant. The values of the derivatives $\frac{\partial F_i}{\partial a_j}$ in (2) are determined for parameters E and λ_p ensuring the minimum of the objective function.

The inverse of the curvature matrix a is the covariance matrix C, i.e.:

$$C_{kl} = [\alpha]_{kl}^{-1} \tag{3}$$

The uncertainties of the identified parameters E and λ_p can be determined as the square roots of the diagonal components of the matrix C, i.e.:

$$u_E = \sqrt{C_{11}}, \quad u_{\lambda p} = \sqrt{C_{22}} \tag{4}$$

Using the experimental results for five membranes prepared with different prestretching forces and Formulas (2)–(4), where the derivatives $\frac{\partial F_i}{\partial a_j}$ were approximated numerically for both membrane models used, the uncertainty values u_E and $u_{\lambda p}$ were determined and given in Table 2.

4.4. Method validation

Validation of the proposed identification method was carried out by

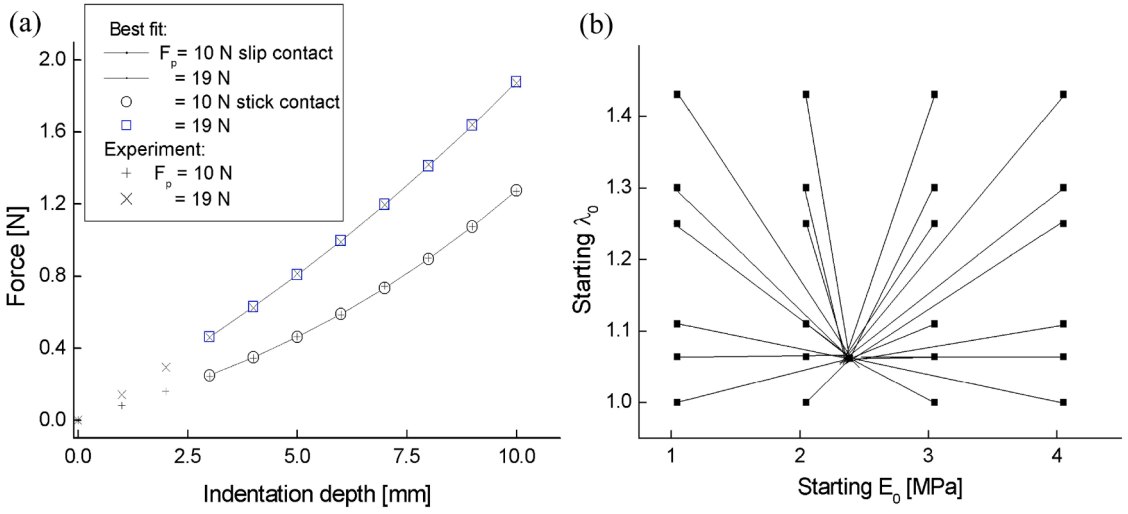

Fig. 8. Example results of fitting the indentation curves by the model with parameters determined for optimization (a) and illustration of the selected identification process with different optimization starting points (b).

Table 2
Uncertainty of the identified parameters: Young's modulus and pre-stretching determined for different membranes and two models of contact.

Pre-stretching force F_P [N]	Slip contact		Stick contact	
	Uncertainty of Young's modulus u_E[kPa]	Uncertainty of pre-stretching $u_{\lambda p}$ [-]	Uncertainty of Young's modulus u_E [kPa]	Uncertainty of pre-stretching $u_{\lambda p}$ [-]
0	47.5	0.00039	54.7	0.00042
5.7	48	0.00055	55.4	0.00059
10.1	47	0.0009	54.0	0.0010
18.3	42.6	0.0023	48.4	0.0025
28	39.9	0.0038	44.9	0.0042

comparing the results of the modeling and indentation tests for the membrane with the liquid under the membrane. The modeling results were obtained using Young's modulus E and the pre-stretch $\lambda_p$values determined from liquid-free membrane tests, as per Table 1, for both the slip and non-slip cases. Selected validation results are shown in Fig. 9 for the membrane with pre-stretching forces of 18 and 28 N.

The graphs show a good convergence of the theoretical predictions with the experimental results. The role of the boundary condition for the contact of the membrane with the indenter does not play a significant role. The comparison shows that the agreement of model predictions and experimental data for force (Fig. 9a) is better than for pressure (Fig. 9b).

4.5. Discussion

The results of the estimation of the Young's modulus (Fig. 6) show a noticeable dispersion of the stiffness modulus values determined for different membranes of the same material, despite the good agreement between the individual model predictions and the indentation test results. The high R^2 values (Table 1) and the good fit of the modeling results and experimental results, an example of which is shown in Fig. 8a, indicate the consistency of the results. Possible reasons for the scattering of the estimated values of the stiffness modulus can be associated with the material or methodology of experimental testing of the membranes, but they can also have a source in the model or identification method used.

The material or experimental causes are inhomogeneity of the starting membrane material or imperfect preparation of the stressed membranes. Due to the friction between the membrane and the tensioning piston (Fig. 1), the uniformity of the pre-stretching is not guaranteed. In turn, the reasons related to modeling are, for example, the incomplete adequacy of the neoHookean model of the material, not taking into account the internal viscosity or deviations from the assumed boundary conditions, in particular for the contact of the indenter and the membrane. Computational problems may result from integration errors of the governing equation system or from ambiguities in the identification procedure.

As part of the research, efforts were made to recognize and limit the impact of the above-mentioned factors on the identification results. Thanks to the use of gluing the membranes to the ring, then deformations or slipping of the membrane from the holder, which may occur in tests of membranes mounted directly in the clamping holder, are limited.

Due to the difficulty of controlling the contact condition between the indenter and the membrane, the identification calculations were carried out for two extreme assumptions, i.e. ideal slip and complete lack of slip. Due to the lack of significant differences between the identification results for both contact conditions, it can be estimated that the role of this factor is insignificant, and each of the intermediate cases in which a partial slip occurs will be within the limits of the results for extreme cases.

The work assumes a model using an incompressible neoHookean material. As a consequence, the relaxation of the pre-stretched membrane and the creep of the membrane under the load of the indenter were omitted. The adoption of these assumptions was associated with the implementation of quasi-static tests and relatively small deformations of the membrane. Further work is needed using other models to assess the impact of these assumptions on the identification results.

The tests of the applied optimization procedure showed that, regardless of the choice of starting point values, the same values of the estimated parameters were obtained (see Fig. 8b). This means that the applied local optimization procedure for minimizing the error function worked well and there was no need to use global optimization methods, which are much more time-consuming. At the same time, it should be added that problems with the convergence of the integration of the model equations for small forces and penetration depth have not been eliminated, and therefore the range of data included in the error function has been limited. Diagnosing and removing the causes of integration problems remains the goal of future research.

Despite the issues of Young's modulus dispersion and its possible causes still requiring further study, it is worth noting that the obtained results are consistent with the data determined in the uniaxial tensile test available in the literature. The results of such tests for small deformations give Young's modulus values from 1.7 to 2.7 MPa [41–43], and for large deformations - values from 0.8 to 1.75 MPa [44–47].

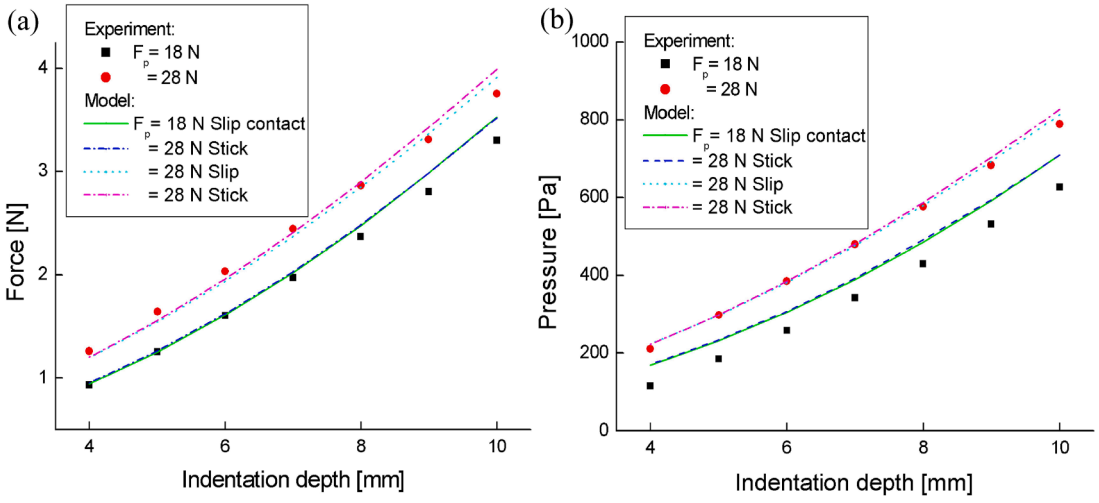

Fig. 9. Comparison of experimental results and model predictions for the force on the indenter (a) and the pressure of the liquid under the membrane (b) depending on the indentation depth. The values of Young's modulus E and pre-stretch λ_p for the model were adopted on the basis of the membrane test without the liquid.

Therefore, the average values of the moduli determined in the indentation test, which are 2.22 MPa for the no-slip condition and 2.36 MPa for the slip condition, are within the range of the Young's modulus values of the uniaxial tensile test in the range of small deformations. It is worth noting that the evaluated uncertainties of Young's modulus and initial stretching, given in Table 2, are much smaller than the differences of these parameters determined from subsequent measurement series (for different *Fp*). The uncertainties are small compared to the values of the parameters themselves. As the pre-tension of the membrane increases, the pre-stretch uncertainty increases significantly while the Young's modulus uncertainty decreases slightly.

It can be noted that instead of using the membrane in an air test to identify the stiffness and pre-stretching, a test with a liquid under the membrane could be used. Different tests have shown, however, that the liquid method is more troublesome at the stand preparation stage, especially when it comes to complete elimination of air from under the membrane. In addition, more significant convergence problems were observed in the developed procedure for the numerical solution compared to the solution for liquid-free membranes. At this stage, this excludes this method from iterative, automated in the optimization code applications for parameter estimation. The model with liquid under the membrane could be used in the identification of some tests on biological materials, such as in the case of examining skin with a soft layer of subcutaneous tissue in the early stage of lymphedema or in the study of cell membranes, if a flat membrane model would be applicable.

Due to the model of the elastic membrane material adopted in the work, the developed identification method applied to polymeric materials relates primarily to quasi-static properties. Such properties, especially stiffnesses, may differ from dynamic properties where internal friction affects the estimated stiffness values [48]. The paper neglects irreversible phenomena such as the dependence of the stress-strain curve on the maximum load in the previous loading cycle (so-called softening of the stress-strain curve), called the Mullins effect [37,38] and plastic deformation of the material. The elastic material model of the membrane is also as simplified as possible (incompressible neoHookean material) and further development of the finite deformation identification method, depending on the type of membrane material, may require, for example, the Mooney-Rivlin model [21,49–51], the Ogden model [50,52–54], the Arrud-Boyce model [53,55], the Yeoh model [56,57] or the Gent model [58,59]. Thus, the discussion in the paper is directed only to the case study analysed, and for other types of materials (elastic or non-elastic) an in-depth study of the material properties of the membrane for specific boundary conditions is required, case by case. Other assumptions of the developed identification method include: a flat indenter and a constant contact surface with the membrane without side contact (other indenter shapes and variable contact surfaces were omitted), an initially flat, circular membrane (the method does not apply, e.g., to cell membranes), no wrinkles on the membrane and its impermeability to liquids (validation tests with water for porous membranes are excluded), incompressibility of the liquid under the membrane. Abandoning the above assumptions requires further work on the method.

5. Conclusions

The methods were presented of determining the Young's modulus of the membrane material and the initial stretching of the membrane based on the results of the indentation test and the solution of the inverse problem. In addition, the method was validated by comparing the results of the simulation of the indentation test of the membrane under which the volume remains constant (the closed space is filled with the liquid) with the experimental results, using the previously determined values of Young's modulus and initial stretch in the simulations. The independent (manipulated) variable in both tests (identification and validation) is the displacement of the indenter. The dependent variable is the force with which the membrane acts on the indenter and, in the case of the validation test, additionally the pressure in the liquid. A latex type elastomer was selected as the test material, the samples of which were prepared with various degrees of pre-stretching. Validation tests showed the agreement of the theoretical predictions with the experimental results. The observed differences were justified by technical problems (preparation of homogeneous samples of stretched membranes, deviations from the ideal implementation of the experiments) or factors not taken into account in the model used.

In the proposed method, the limit for the indentation depth used was assumed to be maximally equal to the diameter of the indenter, which simplifies the modeling of membrane deformation. Relatively large membrane surfaces in the proposed tests compared to the sample surfaces in uniaxial tensile tests reduce the role of material inhomogeneity. By bonding the membrane to the ring, the simple process for preparing samples of pre-stretched materials and the undesirable effects of squeezing the membrane in the holders were eliminated. The above-mentioned aspects give hope that the developed method will be useful in the study of technical materials as well as biological or bio-replacement materials (e.g. leather or artificial bladder walls).

Considering the limitations of the method noted, its further development can be envisaged. In particular, other material models should be considered, e.g. the Mooney-Rivlin model, often used for elastomers, or a model that takes into account the internal friction in the material. Regarding the equipment, it is worth automating the measurement, in particular by adding an appropriate indenter drive (electric motor), microcontroller and software that enables faster setting of the measurement parameters and the convenient acquisition of results. Thanks to this, it will be possible to reduce the step of the indenter and reduce the measurement uncertainty.

CRediT authorship contribution statement

T. Fąs: Visualization, Methodology, Investigation, Data curation. **K. Kazimierska-Drobny:** Visualization, Validation, Investigation. **M. Kaczmarek:** Writing – review & editing, Writing – original draft, Visualization, Supervision, Software, Methodology, Conceptualization.

Declaration of competing interest

The authors declare that they have no known competing financial interests or personal relationships that could have appeared to influence the work reported in this paper.

Data availability

Data will be made available on request.

Appendix A. Model

In order to model the membrane rigidly clamped along the edge at $r=R_e$ at its periphery, loaded axi-symmetrically in the indentation test, we adopted the model of incompressible neoHookean material. Detailed assumptions and equations of the model along with a description of its numerical solution are presented in the paper [36]. The model concerned a membrane without pre-stretch, under which there was an incompressible liquid. Here we present the equations of the model, introducing the effect of pre-stretching and distinguishing two cases: without liquid and with liquid under the membrane, as shown in Fig. A1. In order to take into account the pre-stretch of the membrane, we assumed, in accordance with the concept proposed

in [60], that in the reference configuration to which the formulated description of the membrane refers, initial equi-biaxial stretches were already present.

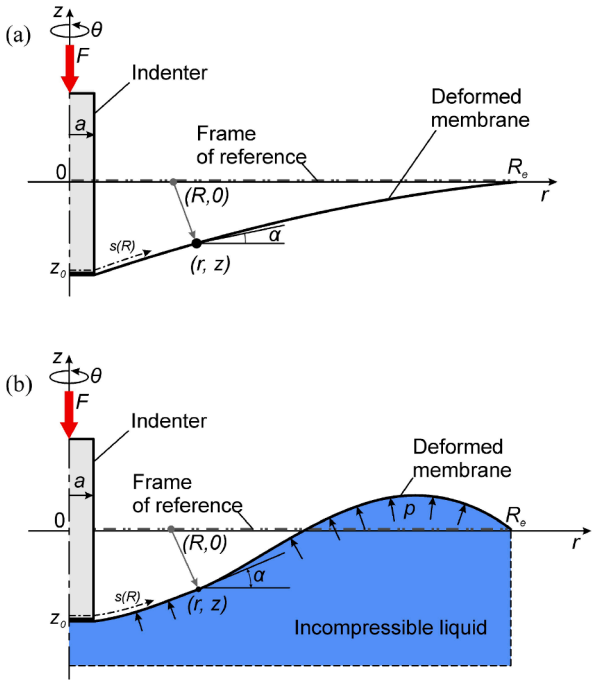

Fig. A1. Membrane deformation during the indentation test without liquid (a) and with liquid under the membrane (b).

In order to model the deformation of the membrane by the indenter, a cylindrical coordinate system (r, ϕ, z) was adopted and the considerations could be restricted to any membrane cross section. The material point originally located in the reference configuration at (R, $z = 0$) was displaced to the point ($r = r(R)$, $z = z(R)$), as shown in Fig. A1. The coordinate s denoted the arc length of the cross-section curve of the deformed membrane. The angle made by the tangent of the cross-section curve at (r, z) with the r axis was α. In the reference configuration the membrane was flat and its center ($R = 0$) lay in the $z = 0$ plane. A cylindrical indenter of radius a located in the axis of the membrane caused its deformation. In the case of the membrane placed on a liquid layer, the volume under the membrane did not change and the shape of the liquid reservoir did not play any role. The pressure in the liquid under the membrane could be expressed as $p = P_0 - \rho g z$, where P_0 was an unknown constant dependent on the membrane deformation and equal to zero for the undeformed state, r was the liquid density, and g denoted the gravitational acceleration. When there was no liquid under the membrane then the pressure was $p = 0$.

The set of equations that describe the finite deformation of the membrane, ignoring its weight, is as follows [36,61,62]:

$$\begin{aligned}
\frac{d\lambda_s}{dR} &= \frac{\lambda_s\left(T_\phi - T_s\right)\cos\alpha - \lambda_\phi\left(\dfrac{\partial T_s}{\partial \lambda_\phi}\right)\left(\lambda_s\cos\alpha - \lambda_\phi\right)}{R\lambda_\phi\left(\dfrac{\partial T_s}{\partial \lambda_s}\right)} \\
\frac{d\alpha}{dR} &= \frac{pR\lambda_s\lambda_\phi - T_\phi\lambda_s\sin\alpha}{R\lambda_\phi T_s} \\
\frac{d\lambda_\phi}{dR} &= \frac{\lambda_s\cos\alpha - \lambda_\phi}{R} \\
\frac{dz}{dR} &= \lambda_s\sin\alpha
\end{aligned} \tag{A1}$$

where λ_s and λ_ϕ are the longitudinal (along the cross-section curve in the r–z plane) and latitudinal (along the direction normal to the r–z plane) principal stretches, respectively:

$$\lambda_s = \frac{ds}{dR}, \lambda_\phi = \frac{r}{R} \tag{A2}$$

where T_s and T_ϕ are the longitudinal and latitudinal line tensions in the deformed configuration, respectively. For the incompressible neoHookean material (the simplest hyperelastic model) of the membrane, the tensions are:

$$\begin{aligned}
T_s &= \frac{Eh_0}{3}\left(\frac{\lambda_s}{\lambda_\phi} - \frac{1}{\lambda_s^3\lambda_\phi^3\lambda_p^6}\right) \\
T_\phi &= \frac{Eh_0}{3}\left(\frac{\lambda_\phi}{\lambda_s} - \frac{1}{\lambda_s^3\lambda_\phi^3\lambda_p^6}\right)
\end{aligned} \tag{A3}$$

where E is the small-strain Young's modulus, h_0 denotes the thickness of the undeformed membrane, and λ_p means an equi-biaxial pre-stretch.

In order to determine the force on the indenter as a function of its penetration depth, a part of the membrane that, in the deformed configuration, is located between the edge of the indenter ($r(R_0) = a$) and the clamping ring (r=R_e) is considered (the radial coordinates of the left and the right boundaries in the reference configuration are R_0 and Re). Given the system of equations (A1), four boundary conditions can be formulated:

(1) The axial coordinate of the left boundary of the membrane in the reference configuration R_0 is:

$$z(R_0) = z_0 \tag{A4}$$

(2) The stretches of the membrane at the indenter edge depend on whether the membrane/indenter contact is a stick or slip type (see [36]). For the stick contact, the condition can be written for latitudinal stretch:

$$\lambda_\phi(R_0) = 1 \tag{A5}$$

For the slip contact the equilibrium condition for the longitudinal line tensions, the continuity of latitudinal stretches, and the homogeneity of the stretches in the plane part of the membrane under the indenter for $R = R_0$ lead to the condition (see [36]):

$$\frac{\left(\lambda_\phi\lambda_p\right)^6 - 1}{\left(\lambda_\phi\right)^3} = \frac{\left(\lambda_s\lambda_p\right)^4\left(\lambda_\phi\lambda_p\right)^2 - 1}{\left(\lambda_s\right)^3}\cos\alpha \tag{A6}$$

where stretches λ_ϕ, λ_s are defined for $R = R_0^+$ (plus sign superscript denotes right-hand limit) and the pre-stretch λ_p has been added compared to the paper [39].

(3) For the clamped edge of the membrane (R=R_e) the axial position is:

$$z(R_e) = 0 \tag{A7}$$

(4) The latitudinal stretch is:

$$\lambda_\phi(R_e) = 1 \tag{A8}$$

In the procedure for solving the model with liquid under the membrane, the requirement that the volume of liquid under membrane V is constant is used to determine the pressure p, i.e.:

$$\Delta V = \int_{R_0}^{R_e} 2\pi r(R)z(R)dR + \pi a^2 z_0 = 0 \tag{A9}$$

In the absence of liquid, it is enough to assume that in the system of equations (A1) $p \equiv 0$ and the boundary conditions (A4)–(A8) do not change.

For a given indentation depth z_0, the force F acting on the indenter may consist of two components: the force due to the stresses in the membrane for $r(R_0) = a$ and, in the presence of a liquid, the resultant force transmitted through the membrane on the surface $r \leq a$, coming from the pressure of the liquid, is:

$$\underline{F} = 2\pi a T_s(R_0)\sin(\alpha(R_0)) + \pi r^2 p(R_0) \tag{A10}$$

In the absence of liquid in Eq. (A10), only the first term remains.

References

[1] Liu KK, Ju BF. A novel technique for mechanical characterization of thin elastomeric membrane. J Phys Appl Phys 2001;34:L91–4. https://doi.org/10.1088/0022-3727/34/15/102.

[2] Ju BF, Wan KT, Liu KK. Indentation of a square elastomeric thin film by a flat-ended cylindrical punch in the presence of long-range intersurface forces. J Appl Phys 2004;96:6159–63. https://doi.org/10.1063/1.1812822.

[3] Liu J, Chen Z, Liang X, et al. Puncture mechanics of soft elastomeric membrane with large deformation by rigid cylindrical indenter. J Mech Phys Solids 2018;112:458–71. https://doi.org/10.1016/j.jmps.2018.01.002.

[4] Garnica-Palafox IM, Álvarez-Camacho M, Sánchez-Arévalo FM. Macro- and micromechanical responses of an elastomeric membrane undergoing biaxial tension by indentation. J Mater Sci 2019;54:14255–74. https://doi.org/10.1007/s10853-019-03887-w.

[5] Kolesnikov AM, Shatvorov NM. Indentation of a circular hyperelastic membrane by a rigid cylinder. Int J Non Linear Mech 2022;138:103836. https://doi.org/10.1016/j.ijnonlinmec.2021.103836.

[6] Liu J, Zhong D, Yin T, et al. Indentation of elastomeric membranes by sphere-tipped indenters: snap-through instability, shrinkage, and puncture. J Mech Phys Solids 2022;167:104973. https://doi.org/10.1016/j.jmps.2022.104973.

[7] Lima-Rodriguez A, Gonzalez-Herrera A, Garcia-Manrique J. Study of the dynamic behaviour of circular membranes with low tension. Appl Sci 2019;9:4716. https://doi.org/10.3390/app9214716.

[8] Zheng Y, Crosby AJ, Cai S. Indentation of a stretched elastomer. J Mech Phys Solids 2017;107:145–59. https://doi.org/10.1016/j.jmps.2017.07.008.

[9] Seekala H, Bathini L, Wasekar NP, et al. A unified approach to quantify the material and geometrical effects in indentation size effect. J Mater Res 2023;38:1740–55. https://doi.org/10.1557/s43578-023-00927-9.

[10] Jones D, Treloar L. The properties of rubber in pure homogeneous strain. J Phys Appl Phys 2001;8:1285. https://doi.org/10.1088/0022-3727/8/11/007.

[11] Brown R. Physical testing of rubber. 4th ed. New York: Springer; 2006.

[12] Zhang MG, Cao YP, Li GY, et al. Spherical indentation method for determining the constitutive parameters of hyperelastic soft materials. Biomech Model Mechanobiol 2014;13:1–11. https://doi.org/10.1007/s10237-013-0481-4.

[13] Lee H, Pharr GM, Nahm SH. Material Property evaluation of hyper-elastic rubber by micro-indentation. In: Proceedings of the SEM annual conference and exposition on experimental and applied mechanics; 2003.

[14] Nguyen N, Wineman A, Waas A. Indentation of a nonlinear viscoelastic membrane. Math Mech Solids 2013;18:24–43. https://doi.org/10.1177/1081286511434196.

[15] Ju BF, Liu KK. Characterizing viscoelastic properties of thin elastomeric membrane. Mech Mater 2002;34:485. https://doi.org/10.1016/S0167-6636(02)00176-X. –49.

[16] Kim JH, Gouldstone A. Spherical indentation of a membrane on an elastic half-space. J Mater Res 2008;23:2212–20. https://doi.org/10.1557/JMR.2008.0278.

[17] Cheng YT, Cheng CM. Scaling, dimensional analysis, and indentation measurements. Mater Sci Eng R Rep 2004;44:91–149. https://doi.org/10.1016/j.mser.2004.05.001.

[18] Lima-Rodriguez A, Garcia-Manrique J, Dong W, et al. A novel methodology to obtain the mechanical properties of membranes by means of dynamic tests. Membranes 2022;12:288. https://doi.org/10.3390/membranes12030288.

[19] Cloonan AJ, O'Donnell MR, Lee WT, et al. Spherical indentation of free-standing acellular extracellular matrix membranes. Acta Biomater 2012;8:262–73. https://doi.org/10.1016/j.actbio.2011.08.003.

[20] Kamper M, Bekker A. Non-contact experimental methods to characterise the response of a hyper-elastic membrane. Int J Mech Mater Eng 2017;12:15. https://doi.org/10.1186/s40712-017-0082-6.

[21] Elkut F, Bradley GR, Krywonos J, et al. Numerical study of the mechanics of indentation bending tests of thin membranes and inverse materials parameters prediction. Comput Mater Sci 2012;52:123–7. https://doi.org/10.1016/j.commatsci.2011.03.025.

[22] Pamplona DC, Weber HI, Sampaio GR. Analytical, numerical and experimental analysis of continuous indentation of a flat hyperelastic circular membrane by a rigid cylindrical indenter. Int J Mech Sci 2014;87:18–25. https://doi.org/10.1016/j.ijmecsci.2014.05.028.

[23] Selvadurai APS, Shi M. Fluid pressure loading of a hyperelastic membrane. Int J Non Linear Mech 2012;47:228–39. https://doi.org/10.1016/j.ijnonlinmec.2011.05.011.
[24] Barenblatt GI, Joseph DD. Collected papers of R.S. Rivlin: volume I and II. New York: Springer; 1997.
[25] Reuge N, Schmidt FM, Maoult YLe, et al. Elastomer biaxial characterization using bubble inflation technique. I: experimental investigations. Polym Eng Sci 2001;41:522–31. https://doi.org/10.1002/pen.10749.
[26] Johnson M, Murphy N, Ekins R, et al. Equi-biaxial fatigue testing of EPM utilising bubble inflation. Polym Test 2016;53:122–31. https://doi.org/10.1016/j.polymertesting.2016.05.017.
[27] Brown R. Physical test methods for elastomers. New York: Springer; 2018.
[28] Keerthiwansa GWR, Javořík J, Kledrowetz J, et al. Elastomer testing: the risk of using only uniaxial data for fitting the Mooney-Rivlin hyperelastic-material model. Mater Technol 2018;52:3–8. https://doi.org/10.17222/mit.2017.085.
[29] Esmail JF, Mohamedmeki MZ, Ajeel AE. Using the uniaxial tension test to satisfy the hyperelastic material simulation in ABAQUS. IOP Conf Ser Mater Sci Eng 2020;888:012065. https://doi.org/10.1088/1757-899X/888/1/012065.
[30] ISO 37. Rubber, vulcanized or thermoplastic Determination of tensile stress-strain properties. 2017.
[31] Hitt DJ, Gilbert M. A machine for the biaxial stretching of polymers. Polym Test 1994;13:219–37. https://doi.org/10.1016/0142-9418(94)90029-9.
[32] Zhao X, Berwick ZC, Krieger JF, et al. Novel design of cruciform specimens for planar biaxial testing of soft materials. Exp Mech 2014;54:343–56. https://doi.org/10.1007/s11340-013-9808-4.
[33] Hu JJ, Chen GW, Liu YC, et al. Influence of specimen geometry on the estimation of the planar biaxial mechanical properties of cruciform specimens. Exp Mech 2014;54:615–31. https://doi.org/10.1007/s11340-013-9826-2.
[34] Hariharaputhiran H, Saravanan U. A new set of biaxial and uniaxial experiments on vulcanized rubber and attempts at modeling it using classical hyperelastic models. Mech Mater 2016;92:211–22. https://doi.org/10.1016/j.mechmat.2015.09.003.
[35] Scott ON, Begley MR, Komaragiri U, et al. Indentation of freestanding circular elastomer films using spherical indenters. Acta Mater 2004;52:4877–85. https://doi.org/10.1016/j.actamat.2004.06.043.
[36] Fąs T, Kazimierska-Drobny K, Kaczmarek M. Indentation of a circular membrane on an incompressible liquid. Acta Mech 2018;229:4779–90. https://doi.org/10.1007/s00707-018-2248-6.
[37] Cantournet S, Desmorat R, Besson J. Mullins effect and cyclic stress softening of filled elastomers by internal sliding and friction thermodynamics model. Int J Solids Struct 2009;46:2255–64. https://doi.org/10.1016/j.ijsolstr.2008.12.025.
[38] Ogden RW, Roxburgh DG. A pseudo–elastic model for the Mullins effect in filled rubber. Proc R Soc Lond Ser Math Phys Eng Sci 1999;455:2861–77. https://doi.org/10.1098/rspa.1999.0431.
[39] BIPM Joint Committee for Guides in Metrology. Evaluation of measurement data Supplement 1 to the "Guide to the expression of uncertainty in measurement" Propagation of distributions using a Monte Carlo method JCGM. 1st ed.101. Paris; 2008.
[40] Balsamo A, Mana G, Pennecchi F. The expression of uncertainty in non-linear parameter estimation. Metrologia 2006;43:396–402. https://doi.org/10.1088/0026-1394/43/5/009.
[41] Santos G, Tavares G, Gasperi G, et al. Mechanical evaluation of the resistance of elastic bands. Rev Bras Fisioter 2009;13:521–6. https://doi.org/10.1590/S1413-35552009000600009.
[42] Niemczura JG. On the response of rubbers at high strain rates. Albuquerque: Sandia National Laboratories; 2010.
[43] So JH, Tayi AS, Güder F, et al. Stepped moduli in layered composites. Adv Funct Mater 2014;24:7197–204. https://doi.org/10.1002/adfm.201401548.
[44] Patterson RM, Jansen CWS, Hogan HA, et al. Material properties of Thera-band tubing. Phys Ther 2001;81:1437–45. https://doi.org/10.1093/ptj/81.8.1437.
[45] Patterson J, Mansfield SA, Olave JC, et al. Mechanical performance of latex and nitrile medical exam gloves under repeated soap and water treatment. Am J Adv Res 2021;5:1–5. https://doi.org/10.5281/zenodo.5112602.
[46] Chandra T, Harahap H, Wangi Y, et al. Physical and mechanical properties of natural rubber latex film (Rubber Dam) products with filler nanocrystal cellulose from peanut shell (Arachis hypogea L.) and synthetic dyes. IOP Conf Ser Mater Sci Eng 2020;801:012091. https://doi.org/10.1088/1757-899X/801/1/012091.
[47] Uchida MC, Nishida MM, Sampaio RAC, et al. Thera-band® elastic band tension: reference values for physical activity. J Phys Ther Sci 2016;28:1266–71. https://doi.org/10.1589/jpts.28.1266.
[48] Prato A, Romeo R, Cuccaro R, et al. Experimental determination of the dynamic elastic modulus of polymeric soft materials in an extended frequency range: a supported free loading-mass method. Measurement 2022;199:111587. https://doi.org/10.1016/j.measurement.2022.111587.
[49] Rivlin RS, Saunders DW. Large elastic deformations of isotropic materials VII. Experiments on the deformation of rubber. Philos Trans R Soc Lond Ser Math Phys Sci 1951;243:251–88. https://doi.org/10.1098/rsta.1951.0004.
[50] Huang H, Tang W, Yan B, et al. Mechanical responses of the periodontal ligament based on an exponential hyperelastic model: a combined experimental and finite element method. Comput Methods Biomech Biomed Eng 2016;19:188–98. https://doi.org/10.1080/10255842.2015.1006207.
[51] Reis AR, Ferreira JPS, Guerra A, et al. Finite element analysis of the epiretinal membrane contraction. Appl Sci 2022;12:2623. https://doi.org/10.3390/app12052623.
[52] Ogden RW, Hill R. Large deformation isotropic elasticity – on the correlation of theory and experiment for incompressible rubberlike solids. Proc R Soc Lond Math Phys Sci 1972;326:565–84. https://doi.org/10.1098/rspa.1972.0026.
[53] Arruda EM, Boyce MC. A three-dimensional constitutive model for the large stretch behavior of rubber elastic materials. J Mech Phys Solids 1993;41:389–412. https://doi.org/10.1016/0022-5096(93)90013-6.
[54] Saavedra Flores EI, Adhikari S, Friswell MI, et al. Hyperelastic axial buckling of single wall carbon nanotubes. Phys E Low Dimens Syst Nanostruct 2011;44:525–9. https://doi.org/10.1016/j.physe.2011.10.006.
[55] Arruda EM, Boyce MC, Jayachandran R. Effects of strain rate, temperature and thermomechanical coupling on the finite strain deformation of glassy polymers. Mech Mater 1995;19:193–212. https://doi.org/10.1016/0167-6636(94)00034-E.
[56] Yeoh OH. Some forms of the strain energy function for rubber. Rubber Chem Technol 1993;66:754–71. https://doi.org/10.5254/1.3538343.
[57] Chagnon G, Verron E, Gornet L, et al. On the relevance of continuum damage mechanics as applied to the mullins effect in elastomers. J Mech Phys Solids 2004;52:1627–50. https://doi.org/10.1016/j.jmps.2003.12.006.
[58] Horgan CO. The remarkable Gent constitutive model for hyperelastic materials. Int J Non Linear Mech 2015;68:9–16. https://doi.org/10.1016/j.ijnonlinmec.2014.05.010.
[59] Sang J, Xing S, Liu H, et al. Large deformation analysis and stability analysis of a cylindrical rubber tube under internal pressure. J Theor Appl Mech 2016;55:177–88. https://doi.org/10.15632/jtam-pl.55.1.177.
[60] Long R, Hui CY. Axisymmetric membrane in adhesive contact with rigid substrates: analytical solutions under large deformation. Int J Solids Struct 2012;49:672–83. https://doi.org/10.1016/j.ijsolstr.2011.11.008.
[61] Long R, Shull KR, Hui CY. Large deformation adhesive contact mechanics of circular membranes with a flat rigid substrate. J Mech Phys Solids 2010;58:1225–42. https://doi.org/10.1016/j.jmps.2010.06.007.
[62] Libai A, Simmonds JG. The nonlinear theory of elastic shells. 2nd ed. Cambridge: Cambridge University Press; 1998.